The β-Spherulite Morphology of Isotactic Polypropylene Investigated by Raman Spectroscopy

J. Martin, P. Bourson, A. Dahoun, J. Hiver

The β-spherulite morphology of isotactic polypropylene investigated by Raman spectroscopy

J. Martin[1], P. Bourson[1*], A. Dahoun[2], J.M. Hiver [2]

[1] Laboratoire Matériaux Optique Photonique et Systèmes, Université Paul Verlaine de Metz et Supélec, UMR CNRS 7132, 2 rue E. Belin, 57070 Metz, France

[2] Institut Jean Lamour, Département SI2M, UMR CNRS 7198, Nancy Université et Ecole Nationale Supérieure des Mines de Nancy, Parc de Saurupt, 54042 Nancy, France

* Author to whom correspondence should be addressed

Abstract

Raman spectroscopy is used to investigate the α- and β-crystalline polymorphs of isotactic polypropylene. Raman spectra of the polymorphs show some minor differences, in particular the wavenumber shifting of certain scattering bands, which reflect the environment of an isolated macromolecular chain within the packing unit cell of the different crystal forms. For example, the shifting of the 842 cm^{-1} scattering band, which the most susceptible band to cause intermolecular interactions, is used to generate a structural map of one β-spherulite among α-spherulites with a well-defined resolution. Anisotropy of the crystalline phase orientation within a β-spherulite is also investigated by performing polarized Raman spectroscopy measurements. Differences in the polarized spectra are then finely exploited to map the radial lamellae orientation distribution within one β-spherulite.

Keywords: Raman spectroscopy, Isotactic polypropylene, Crystalline polymorphs, Lamellae orientation

1. Introduction

Crystalline morphology of semi-crystalline polymers controls the ultimate properties of the material.[1] Polymorphism is one of the most important aspects of it. Isotactic polypropylene (noted IPP) have three different crystalline polymorphs referred to as the α-, β-, γ- and one liquid crystal form named smectic phase.[2-4] All have been identified by X-ray scattering. Crystallization of each depends strongly on the thermo-mechanical conditions of cooling.[5] The predominant α-form presents a monoclinic unit cell structure and is principally obtained under typical industrial conditions.[6,7] The β-form shows an hexagonal unit cell structure and its appearance is favored under conditions of shear stress and the use of nucleating agents.[3,8,9] The γ- and smetic forms are identified as a triclinic and a pseudo-hexagonal unit cell structure respectively and have a minor occurrence.[10-12] The individual chains in all the crystalline forms have a 3_1 helical conformation with three monomer units per helix.

Vibrational analysis of semi-crystalline polymer, such as InfraRed (IR) or Raman spectroscopy, are particularly well-adapted for the characterization of the overall chain structure regularity because IR absorption and Raman scattering spectra are sensitive to intra-molecular interactions.[13] For example, Snyder et al.[14] shows that it is possible to distinguish unambiguously the three isomeric configurations of polypropylene with Raman spectroscopy. Minogianni et al.[15] and Gatos et al.[16], which exploited the Raman sensibility to IPP 3_1 helical conformation, propose a spectral criterion of the crystallinity degree. On the contrary, it is often assumed that inter-molecular interactions between neighbouring polymer chains in the crystal lattice can be ignored since IR absorption and Raman scattering spectra are insensitive to the lateral order of the crystalline phase.[17] Thus, a handful of works have compared the different crystalline polymorphs of IPP. Results collected by Beckett et al.[18] and Goldstein et al.[19] on far-IR experiments show absorption band splitting which is discussed in terms of inter-molecular vibrational coupling within the crystal unit cell. Chalmers et al.[20] tend to review Raman band shifting noted for the α-, β-, γ- and smetic

polymorphs of IPP in a large wavenumber range of about 40 – 3100 cm^{-1}. In recent papers Ellis et al.[21,22] have used the minor differences noted between the mid-IR spectra of the α- and β-IPP forms to generate maps of β-spherulites. Images obtained have a poor resolution related to the low spatial resolution of IR micro-spectroscopy (10-15 μm).[23] Same authors have performed high-resolution IR micro-spectroscopy experiments using synchrotron IR sources and show an enhancement of the image resolution.[24] By contrast, it is easier to achieve a beam waist of better than 1 μm in Raman micro-spectroscopy by the use of visible laser sources and microscope objective lens.

In this paper we identify differences between the Raman spectra of the α- and β-polymorphs of IPP and used them to construct structural maps of the crystalline morphology with high resolution. In a second part, we focus our attention to crystalline anisotropy in such structures.

2 Experimental

2.1 Material

The used IPP was manufactured and processed by Atochem (ref.: 3050 MN1). The isotactic grade has a broad molecular weight distribution, as assessed by gel permeation chromatography, with $\overline{M}_w$ = 75940 g/mol and $\overline{M}_n$ = 262200 g/mol. Pellets of the polymer were subsequently processed by intrusion in a thick rectangular mould (300 x 200 x 15 mm). This technique consists in slowly extruding the melt at a temperature of 230 °C in the mould maintained at 30 °C feeding under the extruding pressure of 6 MPa during the cooling sequence (240 s). Thermo-mechanical conditions of the intrusion process lead to a predominant α-spherulitic morphology but also favor β-spherulites crystallization in the inner region of the plate as it is seen schematically in Fig. 1. To make sure of the presence of the β-spherulites, external and internal regions are independently characterized by X-ray scattering experiments using the K_α radiation of copper (λ = 0.1542 nm). Patterns are recorded at room temperature with a Philips Geiger counter X-ray diffractometer at 1degree per minute over a 2θ Bragg's angle range of 10-40 degrees. X-ray patterns of the Fig. 2 show that external regions are only composed of α-spherulites since scattering bands located at

2θ = 14.12, 16.9, 18.52, 21.28, 21.80 and 21.86 degrees are attributed to the α-(110), α-(040), α-(130), α-(111), α-(131) and α-(041) crystallographic planes of the α-monoclinic crystal lattice respectively.[8] Apparition of the scattering band located at 2θ = 16.2 degrees corresponding to the β-(300) crystallographic plane of the β-hexagonal crystal lattice indicates the presence of both α- and β-spherulites in the inner region.

2.2 Polarized light microscopy

Polarized light microscopy is used both to observe the polymorphic morphology of the intruded isotactic polypropylene material (shape, size and type of spherulites) and to isolate one particular β-spherulite for its later Raman mapping. All micro-photographs are captured by a CCD camera surmounting an Olympus microscope (model AX 70). Last one works in light transmission configuration and is equipped of a set of two crossed polarizers allowing study of birefringent crystals such as spherulites of IPP.[25,26] Samples observed consist in thin slices of about 30 µm cutted out from the intruded plates as the Fig. 1 shows it. A rotary microtome, developed by Leica (model JUNG RM 2055), is used for sectioning the plate. Slices are then carefully disposed between two cover glasses before their observation.

2.2 Raman micro-spectroscopy

All Raman scattering measurements are carried out on an Aramis® micro-spectrometer developed by Horiba Jobin Yvon (Lille, France). A diode laser emitting a 785 nm exciting line is used and allows a substantial reduction in fluorescence. The system is equipped with a liquid nitrogen cooled, 2000 x 256 pixels CCD detector (Synapse, Horiba Jobin Yvon). All spectra are recorded in back-scattered geometry using a 1200 grooves.mm^{-1} as the diffraction grating and a spectral resolution of 0.6 cm^{-1} is achieved. Raman spectra were calibrated using the neon emission spectrum. The useful spectrum under consideration is ranging from 750 cm^{-1} to 1550 cm^{-1}. Both the incident and scattered lights are collected through an Olympus confocal microscope (x 100 dry objective lens, total magnification x 1000, numerical aperture NA = 0.9 and hole aperture 80 µm).

In this configuration, the lateral and the axial space resolution is about 0.8 µm and 1 µm respectively. When the laser beam is focus onto the sample, the illumination power is ranged between 15 and 20 mW. Rayleigh scattered light is blocked by using a holographic Notch filter. A set of two polarisers is also installed on the spectrometer and offers the possibility to polarize both the incident and the scattered radiation independently. All Spectra are recorded with the Labspec® acquisition software developed by Horiba Jobin Yvon (Lille, France). A personal fitting least-square procedure based on a Lorentzian function adjustment is used to process spectral data and gives access to the useful position, full width at half maximum and integrated intensity of peaks.

Mapping of the crystalline morphology is performed on a selected area of 185 µm x 180 µm using a point-by-point scanning mode with a step size of 1 µm. Acquisition time is about 1 s which correspond to a total measurement time around 10 hours for 33300 spectra individually collected. Two mapping are performed:

- A first one is carried out without polarization of the incident and scattered radiation.

- A second one is performed by maintaining constant polarization geometry, marked VV, where the polarization direction of the incident radiation is parallel to the polarization direction of the scattered radiation.

3. Results and discussion

3.1 Differentiation of α- and β-polymorphs

Fig. 3 shows a polarised optical microphotograph of an area containing both α- and β-spherulites of IPP. The bright structure in the centre of the microphotograph corresponds to a β-spherulite because hexagonal structure of iPP present a high and a negative birefringence.[25,26] This β-spherulite is surrounded by many darker α-spherulites which is related to the biaxial lamellae orientation within the monoclinic structure.[27] Average diameters of the α- and β-spherulites are around 30 µm and 60 µm respectively. Fig. 4 shows Raman spectra consecutively

recorded on a α- and β-spherulite in the range of 750 – 1500 cm^{-1}. Spectra are very similar to each other and differences are subtle. Only very small wavenumber shifts in a number of Raman scattering bands can be observed. Intensity changes in the spectra are not taking into account in this paper. Band shifting is particularly illustrated in Fig. 5 for one Raman band located at 842 cm^{-1} and principally assigned to the rocking mode of the CH_2 alkyl group.[13,14] A shift of about 1 cm^{-1} is noted between the α- and the β-spherulite. The shift noted for all bands (Tab. 1) does not exceed 1 cm^{-1}. This is not surprising because the 3_1 helical conformation of the iPP chains in each crystal remains identical leading to identical intra-molecular interaction energies. Spectra only differ in that helices have not the same lateral steric environment which influences the vibrational motions of the chemical bonds. All the bands which exhibit a shift are assigned in part with a specific Raman vibrational mode of the lateral alkyl groups (CH_2, CH_3) of the IPP monomer.[13,14] Authors such as Beckett and al.[18] and Goldstein and al.[19],who used principally IR spectroscopy, confirm that the pendant methyl group CH_3 is clearly the most susceptible to generate inter-molecular interaction. One can safely assume that the observed wavenumber shift of the Raman bands are due to the crystallographic changes between a α-IPP monoclinic and a β-IPP hexagonal unit cell rather than thermo-mechanical effects during the crystallization sequence. Eventual compressive (and / or extensional) residual stresses at the spherulite boundaries which could appear during the sequential growth are relaxed by the amorphous phase.[28] This is comforted by Gatos et al.[16] who show a higher amount of amorphous phase at the circumference of the α-spherulites than in their centre.

On the basis of the results obtained, attention is focused on the shift of the 842 cm^{-1} band. This is followed over an area of 185 µm x 180 µm delimited by the black box, marked A, on the microphotograph of the Fig. 3. Experimental conditions of the mapping are previously described in the experimental part of the study. Fig. 6 presents the two-dimensional evolution of the 842 cm^{-1} band shifting over the considered area. As expected this evolution generates an image representative of the crystalline morphology of two polymorphs of IPP. It is noted that the correlation between the polarised optical micrograph and the Raman structural map is good because shape and size of the

β-spherulite are respected. Contour of the β-spherulite is well-marked showing its characteristic concave edges. Similar correlations can be made with other bands which exhibit a band shifting as noted in Tab. 1.

3.2 Morphological anisotropy within a β-spherulite

As the Fig. 7 shows it, many spectra are recorded at fixed distance and at variable angle ϕ from the nucleus of one β-spherulite. Measurements are performed using polarization of both the incident and the scattered radiation. The polarization direction of the incident radiation is parallel to the polarization direction of the scattered one (configuration marked VV). Fig. 8 shows the Raman spectra recorded at two extreme angular positions ϕ = 0 and 90 degrees in the range of 960 – 1010 cm^{-1}. Intensity of the bands located at 973 cm^{-1} and 998 cm^{-1} is modified as a function of the angular position. The first band is assigned principally to the C-C asymmetric stretching mode of the skeletal backbones while the second is referred to the rocking mode of the CH_3 lateral alkyl groups.[13,14] For ϕ = 0 degree, it is seen that band at 973 cm^{-1} is dominant while band at 998 cm^{-1} is weak. For ϕ = 90 degrees, the band at 973 cm^{-1} has a minor intensity with respect to the band at 998 cm^{-1}. Observations have to be related to the crystalline lamellae orientation within a β-spherulite.[25,26,33,34] As the schematic diagram of the Fig. 9 shows it, **c**-axis of the lamellae at ϕ = 0 degree (equatorial region) is parallel to the direction of polarization VV. In this case, Raman scattering is excited principally from the *C-C* skeletal backbones explaining the high value of the 973 cm^{-1} band intensity.[29-32] Simultaneously, Raman scattering produced from the CH_3 lateral alkyl groups is less activated which explains the low value of the 998 cm^{-1} band intensity. This tendency is completely inversed when the **c**-axis of the lamellae at ϕ = 90 degrees (polar region) is perpendicular to the direction of polarization. It appears that the ratio I(973) / I(998) of these two bands intensity can be used as a Raman criterion of the lamellae orientation of IPP. Fig. 10 presents this ratio evolution I(973) / I(998) in function of the angular position in the β-spherulite considered (Fig 7) and a periodic variation is observed confirming the radial orientation distribution of lamellae

within a β-IPP spherulite. Maxima correspond to lamellae in equatorial region of the β-spherulite while minima are attributed to lamellae in polar region of it (Fig. 9).

Fig. 11 presents the mapping of a β-spherulite by following the evolution of the ratio I(973) / I(998) (black box marked B in Fig. 7). Equatorial, diagonal and polar region are well-delimited. This structural image remind the well-known Maltese-cross extinction obtained on a β-spherulite using polarized optical microscopy.[25,26,33-35]

4. Conclusions

The measurements performed in this study demonstrate that Raman spectroscopy allows differentiating the α- and β-crystalline polymorphs of IPP. Explanation of the subtle differences noted between the Raman spectra of α- and β-forms has to be related to the inter-molecular interactions which are different in each crystal lattice. Spectral differences can be exploited to generate a well-resolved image of the crystalline polymorphs. Moreover, Raman spectroscopy in one polarized configuration is applied to develop a spectral criterion of the lamellae orientation in IPP. This criterion is then used to image the crystalline orientation anisotropy within a β-spherulite and confirms experimentally the radial distribution of lamellae.

Contrary to other techniques as infra-red spectroscopy and X-ray scattering, acquisition times are reduced and spatial resolution (1 μm) is considerably enhanced.

References

1. I.M. Ward, *Mechanical Properties of Solid Polymer*, Eds. (Wiley-Interscience, London, 1971)

2. S.Z.D. Cheng, J.J. Janimak and J. Rodriguez, "Crystalline structures of polypropylene homo- and copolymers", in *Polypropylene: Structure, Blends and Composites*, J. Karger-Kocsis, Eds.(Chapman & Hall, London, 1995), Vol. 2, Chap. 2, p. 31.

3. B. Lotz, J.C. Wittmann and A.J. Lovinger, Polymer **37,** 22, 4979 (1996)

4. B. Fillon, A. Thierry, J.C. Wittmann and B. Lotz, J. Polym. Sci. **31**, B, 1407 (1993)

5. J. Varga, "Crystalline, melting and supermolecular structure of isotactic polypropylene", in *Polypropylene: Structure, Blends and Composites*, J. Karger-Kocsis, Eds. (Chapman & Hall,London, 1995), Vol. 2, Chap. 3, p. 56.

6. G. Natta and P. Corradini, Nuovo Cimento Suppl. **15**, 40 (1960)

7. A. Turner-Jones, J.M. Aizelwood and D.R. Beckett, Makromolek. Chem. **75**, 134 (1964)

8. A. Turner-Jones and A.J. Cobbold, J. Polym. Sci. **6,** B, 539 (1968)

9. S.V. Meille, D.R. Ferro, S. Brückner, A.J. Lovinger and F.J. Padden, Macromol. **27**, 2615 (1994)

10. A. Turner-Jones, Polymer **12**, 487 (1971)

11. B. Lotz, S. Graff and J.C. Wittmann, J. Polym. Sci. **24,** B, 2017 (1986)

12. P.B. McAllister, T.J. Carter and R.M. Hinde, J. Polym. Sci. **16**, 49 (1978)

13. H.Tadokoro, M. Kobayashi, M. Ukita, K. Yasufuku, S. Murahashi and T. Torii, J. Chem. Phys., **42,** 4, 1432 (1965)

14. R.G. Snyder and J.H. Schachtschneider, Spectrochim. Acta. **20**, 853 (1964)

15. C. Minogianni, K.G. Gatos, C. Galiotis, Applied Spectrosc. **59**, 9, 1141 (2005)

16. K.G. Gatos, C. Minogianni, C. Galiotis, Macromol. **40**, 4, 786 (2007)

17. P.C. Painter, M.M. Coleman and J.L. Koenig, *The Theory of Vibrational Spectroscopy and Its Application to Polymeric Materials*, Eds. (Wiley-Interscience, New York, 1982), Chap. 11, p. 227

18. D.R. Beckett, J.M. Chalmers, M.W. Mackenzie, H.A. Willis, H.G.M. Edwards, J.S. Lees and D.A. Long, Eur. Polym. J. **21,** 10, 849 (1985)

19. M. Goldstein, M.E. Seeley, H.A. Willis and V.J.I. Zichy, Polymer **14**, 530 (1973)

20. J.M. Chalmers, H.G.M. Edwards, J.S. Lees, D.A. Long, M.W. Mackenzie and H.A. Willis, J. Raman Spectrosc. **22**, 613 (1991)

21. G. Ellis, M.A. Gómez and C. Marco, Int. J. Vibr. Spectrosc. **5,** 4, 7 (2001)

22. G. Ellis, Macromol. Symp. **184**, 37 (2002)

23. J. Kressler, R. Schäfer and R. Thomann, Appl. Spectrosc. **52**, 10, 1269 (1998)

24. G. Ellis, C. Marco and M.A. Gómez, Infrared Phys. Tech. **45**, 349 (2004)

25. B. Wunderlich, *Macromolecular Physics: Crystal structure, Morphology, Defects*, Eds. (Academic Press, New York, 1973), Chap. 3, p. 313

26. R.J. Samuels and R.Y. Yee, J. Polym. Sci. **10**, 385 (1972)

27. F.J. Padden, H.D. Keith, J. Applied Phys. **44**, 1217 (1973)

28. L.R.G. Treloar, *The Physics of Rubber Elasticity*, Eds. (Clarendon, Oxford, 1975)

29. D.I. Bower, J. Polym. Sci. **10**, 2135 (1972)

30. L.D. Cambon and D.V. Luu, J. Raman Spec. **14**, 291 (1983)

31. L.D. Cambon, J.L. Ramonja and D.V. Luu, J. Raman Spectrosc. **18**, 129 (1987)

32. M. Arruebarrena de Baez, P.J. Hendra and M. Judkins, Spectrochim. Acta **51**, A, 2117 (1995)

33. J.M. Schultz, *Polymer Materials Science*, Eds. (Prentice-Hall, Englewood Cliffs, 1974), Chap.3, p. 154

34. M. Aboulfaraj, B. Ulrich, A. Dahoun, C. G'Sell, Polymer **34**, 4817 (1993)

35. E. Weynant, J.M. Haudin and C. G'Sell, J. Mater. Sci. **15**, 2677 (1980)

List of tables

List of figures

Figure 10: Ratio I(973) / I(998) of integrated intensity of the 973 cm^{-1} and 998 cm^{-1} bands versus measurement angle.

Figure 11: Raman imaging of the lamellae orientation anisotropy within one β-IPP spherulite. The map (190 µm x 180 µm) is constructed using the I(973) / I(998) band ratio.

Table 1: Observed Raman frequencies (cm^{-1}) for α and β polymorphic forms of IPP

Polymorph	**frequency (cm^{-1})**							
α-IPP	809	835	842	900	940	974	998	1037
β-IPP	810	834	843	901	940,5	974,5	998,5	1037
α-IPP	1043	1103	1152	1168	1220	1255	1296	1306
β-IPP	1043	1103	1152,5	1169	1220	1256	1296	1306
α-IPP	1331	1360	1375	1437	1459			
β-IPP	1332	1360	1377	1437	1459			

Figure 1: Schematic diagram of the microtomed slice used in the study and cutted from an IPP intruded plate.

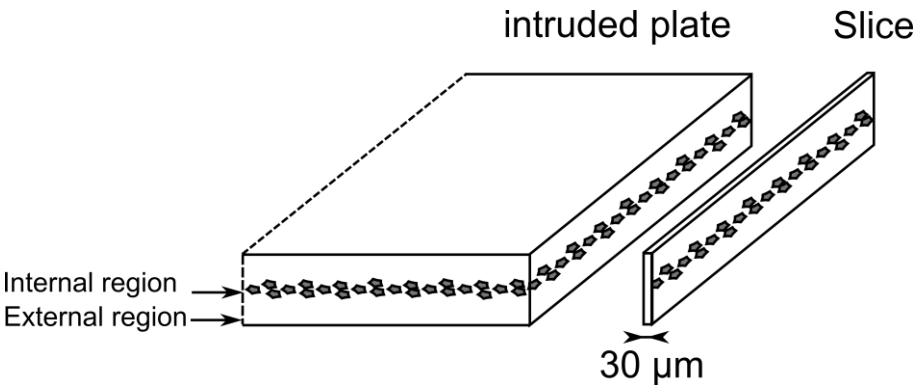

Figure 2: X-ray scattering diagrams of the internal (----) and external (—) region of the IPP intruded plate.

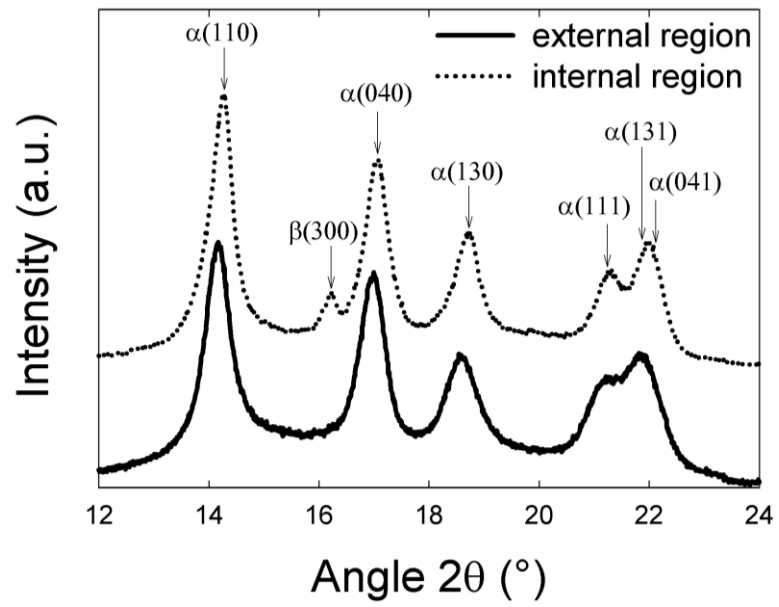

Figure 3: Polarized optical microphotograph of α and β-IPP spherulites. The box marked A corresponds to the mapped zone described in Fig. 6.

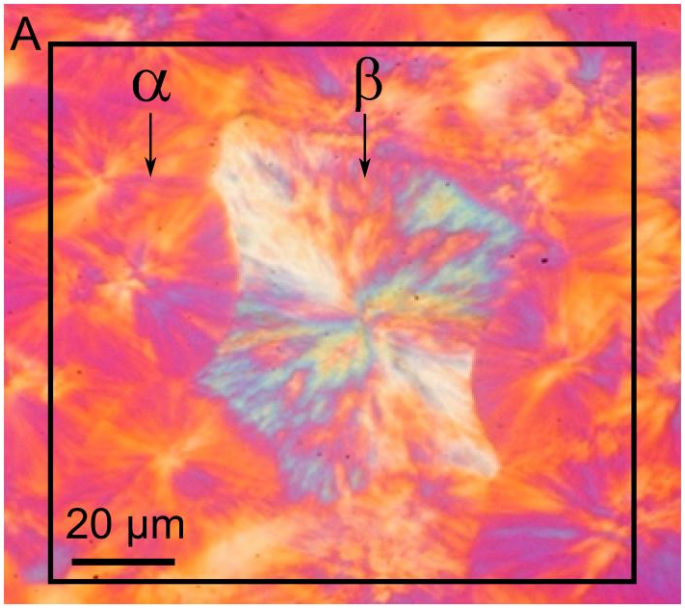

Figure 4: Individual Raman spectra recording on a α and β-IPP spherulites, in the range of 750 – 1550 cm^{-1}.

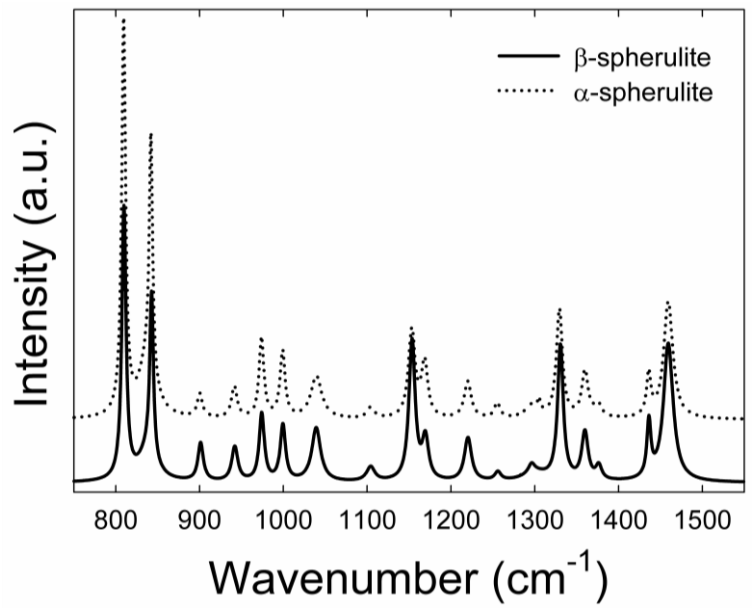

Figure 5: Individual Raman spectra recording on a α and β-IPP spherulites, in the range of 825 – 860 cm^{-1}.

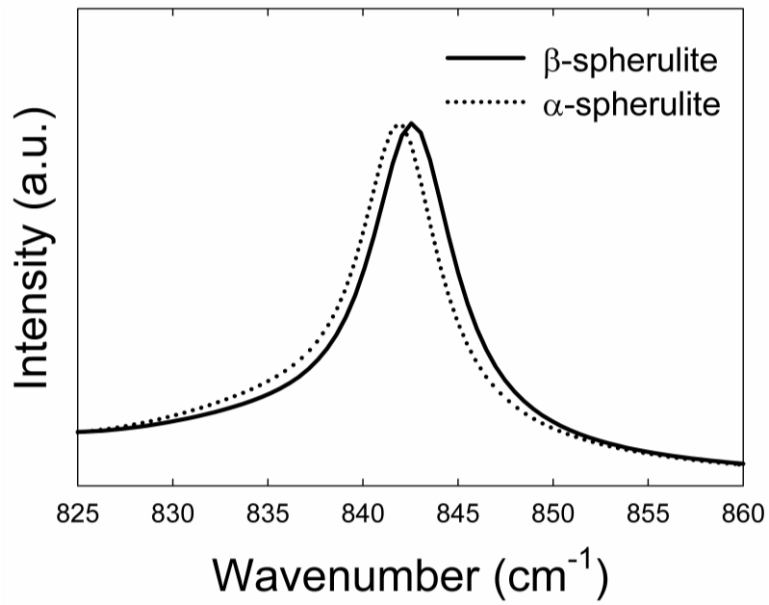

Figure 6: Raman imaging of one β-IPP spherulite surrounded of α-IPP spherulites. The map (185 µm x 180 µm) is constructed using the 842 cm^{-1} band shifting.

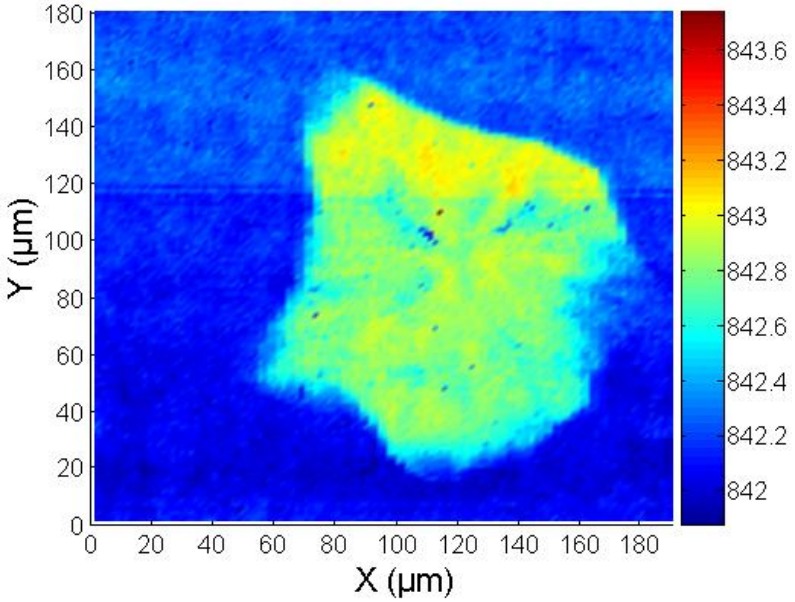

Figure 7: Polarized optical microphotograph of α and β-IPP spherulites. Experimental arrangement for single point spectra taken within the β-IPP spherulite remaining a constant direction of light polarisation VV. The box marked B corresponds to the mapped zone described in Fig. 11.

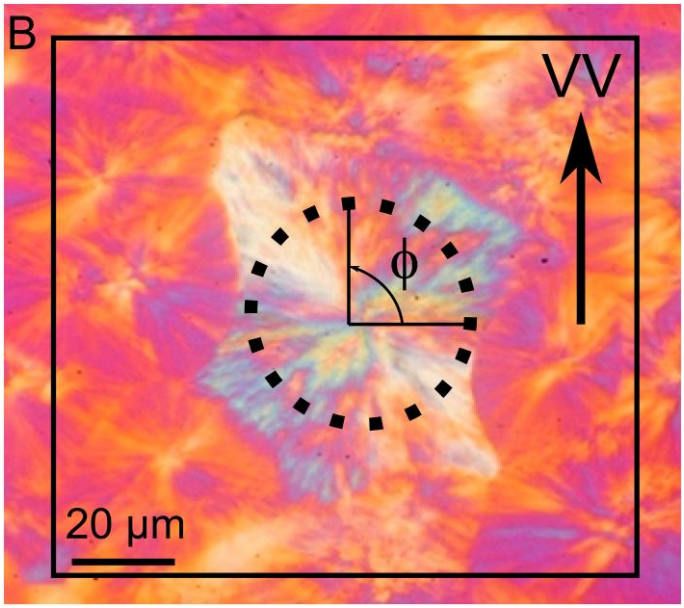

Figure 8: Polarized Raman spectra recorded at angles ϕ = 0 and 90 degrees on a β-IPP spherulite in the range of 960 – 1010 cm^{-1}.

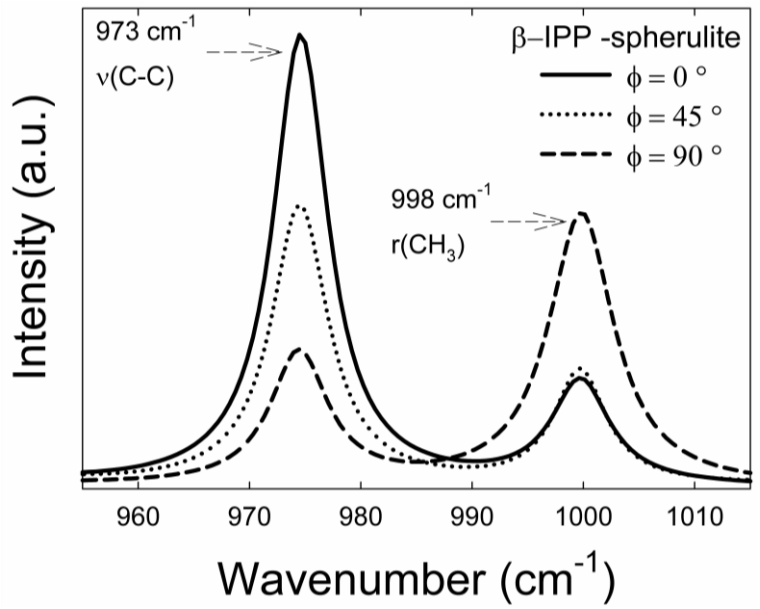

Figure 9: Schematic diagram of lamellae orientation distribution within a β-IPP spherulite with respect to the light polarization marked VV.

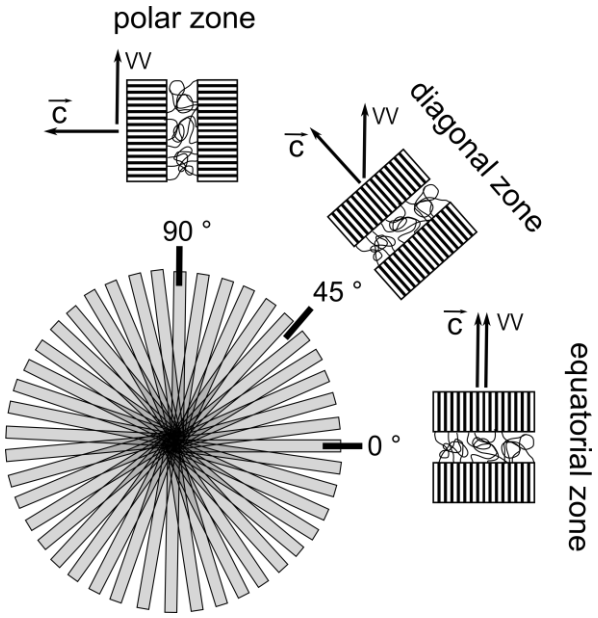

Figure 10: Ratio I(973) / I(998) of integrated intensity of the 973 cm^{-1} and 998 cm^{-1} bands versus measurement angle.

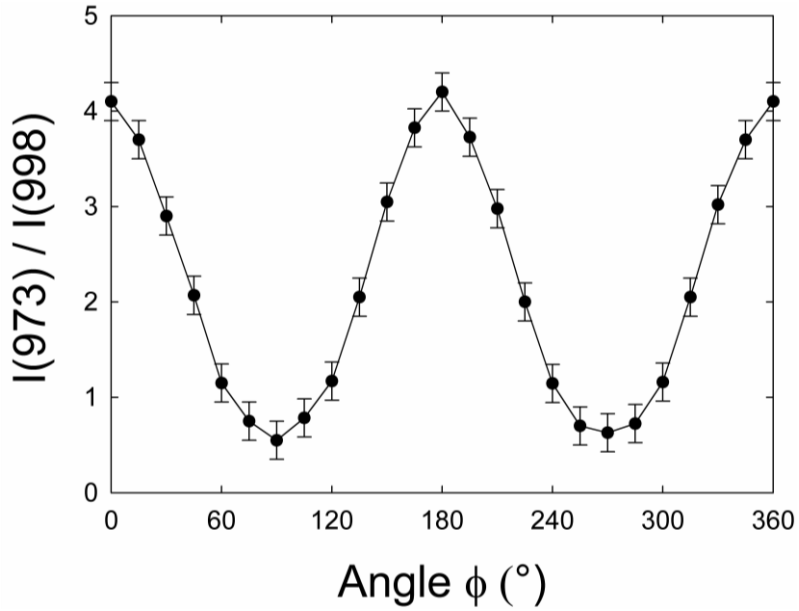

Figure 11: Raman imaging of the lamellae orientation anisotropy within one β-IPP spherulite. The map (190 µm x 180 µm) is constructed using the I(973) / I(998) band ratio.